Journal of Applied Polymer Science

Mechanical and thermal properties of modified kaolin clay/unsaturated polyester nanocomposites

Manoj George,[1] George Elias Kochimoolayil,[2] Jayadas Narakathra Haridas[1]
[1]School of Engineering, Cochin University of Science and Technology, Kochi, Kerala, 682022, India
[2]Department of Polymer Science and Rubber Technology, Cochin University of Science and Technology, Kochi, Kerala, 682022, India
Correspondence to: M. George (E-mail: manojgeorgek@gmail.com)

ABSTRACT: The improvement in thermal and mechanical properties of Nanocomposites prepared with unsaturated polyester (UP) as polymer matrix and various loadings of amino-modified nano kaolinite clay as filler has been studied. Mechanical stirring and ultrasonication resulted in better dispersion of the clay. For curing polyester resin, cobalt naphthenate was used as accelerator and MEKP as initiator. Dynamic Mechanical Analysis (DMA) was carried out to find storage and loss modulus. Thermal stability was found through thermogravimetric analysis and the evaluation of structure and morphology of the nanocomposites were done through XRD, SEM, and TEM. Nanocomposite with 3 phr of amino modified clay has shown higher storage modulus and an improved thermal stability of UP/clay nanocomposites has been established. Tensile strength and toughness of the composite have been found to achieve maximum values at 1 phr of clay and the storage modulus has had an improvement of 38% compared to neat UPR. © 2015 Wiley Periodicals, Inc. J. Appl. Polym. Sci. **2016**, *133*, 43245.

KEYWORDS: clay; mechanical properties; morphology; nanostructured polymers; thermogravimetric analysis

Received 1 August 2015; accepted 19 November 2015
DOI: 10.1002/app.43245

INTRODUCTION

Polymers are considered as the backbone of many modern industries as they can often be replaced some of the metals with improved performance in many critical areas. In three aspects nanocomposite differ from micro composite. Nanocomposite contain small amount of fillers, filler particle size is in nano-range and the filler-polymer interfacial area is large. With small amount of fillers with high aspect ratio the entire polymer is converted into an interfacial polymer with desirable properties.[1] They do exhibit excellent mechanical[2] properties on comparison with those of microcomposites, even with small quantity of nanofillers. They also exhibit increased thermal,[3] chemical,[4] and electrical[5] properties. When compared with conventional composites, they show increased modulus and strength,[6] toughness,[7] decreased permeability,[8,9] higher glass transition temperature (Tg),[10] shrinkage,[11] thermal stability,[12,13] and better dynamic modulus[14] also is observed in polyester/Clay nanocomposites.

Polyester resins possess a wide range of properties such as low cost, strength, stiffness, processability, and chemical resistance, but for many engineering applications, the mechanical properties possessed by the polyester–polymer matrix is not enough. One of the objective of the work is to enhance the mechanical properties of the polyester by adding nanofillers to the resin.[15,16] Second objective is to obtain better dispersion of nanoclay platelets in the resin. For better dispersion of the clay mechanical shearing and ultrasonication is used.[17] Ultra Sonication also aids in the collapse the air bubbles entrapped in the resin during mechanical shearing. Moreover though there are many works that deals with montmorillonite clay composites, only very few are available for composites with kaolin clay as filler in unsaturated polyester as resin.[18,19]

The polymer nanocomposite used in this work is prepared with unsaturated polyester (UP) as polymer matrix with amino-modified nano kaolinite clay as filler. Nano kaolinite clay is basically layered-type alumina silicate. For curing unsaturated polyester, cobalt naphthenate was used as accelerator and MEKP as initiator. In the thermoset industry, UP resins are widely used as the matrix material, almost up to three-fourth of the total volume.[20] These UP resins are mainly utilized owing to their commendable mechanical, chemical, thermal, and electrical properties. In addition, they are less expensive when compared with other resins and their handling and processing is fairly easy, making the most favorable option in the thermoset industry. After the addition of required fillers, they can be used in various molding methods like Resin Transfer Molding, hand lay-up, and spray-up.

© 2015 Wiley Periodicals, Inc.

Kaolin clay derived its name from Kao-Ling a locality in Jianxi, China. The chemical formula for kaolinite is $Al_2[Si_2O_5]$ $(OH)_4$. Its structure consists of silicate (Si_2O_5) layers bonded to aluminum hydroxide ($Al_2(OH)_4$) layers called gibbsite.[21] Kaolinite layer consists of an alumina octahedral sheet and a silica tetrahedral sheet. Silicate tetrahedral sheet are linked in the shape of hexagonal array. The adjacent layers are connected by hydrogen bonds and van der Waals forces. This interlayer induces limited access to the inter lamellar aluminol groups (Al–OH), which can further be utilized for grafting reactions. The hydroxyl group, the most reactive functional group in kaolinite, is capable of part-taking in numerous chemical reactions and ion exchange processes.[22]

Thus for making the nanoclay surface hydrophobic, the inorganic cations present in galleries are exchanged with organic cationic surfactants like, alkylammonium or alkylphosphonium, having long aliphatic chains.[23] The organic modification does not only impart hydrophobic character but also causes increased interlayer spacing and decreased surface energy of the clay platelets.[24] Larger the gallery spacing and weaker the interaction forces easier would be the exfoliation and distribution of the clay layers in the polymer matrix. The cationic surfactants also provide functional groups, which interact with the polymer or initiate polymerization and therefore increase interfacial interactions, another advantage of organo clays making them preferred over unmodified clay for polymer/clay nanocomposites.

Much of the work in UP nanocomposites is done using montmorillonite and silica Relatively few reports are available with kaolin clay and hence in our study, instead of montmorillonite, kaolin clay with a 1 : 1 type layered structure with chemical composition $Al_2Si_2O_5$ $(OH)_4$ is used.[25,26] Thus amino silane modified kaolin clay (Nanocaliber 100A) is used as the filler in this study.

EXPERIMENTAL

Materials

Unsaturated Polyester. UP was purchased from Aiswarya polymers, Coimbatore, India AIPOL-1102. It is a general purpose laminating resin with light yellow color with viscosity in the range 200–350 cp at 25°C. It shows a gel time between 5 to 9 min.

Kaolin Clay. The sample selected for the experiment is amino silane modified kaolin clay (Nanocaliber100A-N100A), provided by English India Clays Limited, Thiruvananthapuram, India. The Nanocaliber100A-N100A has the following characteristics, plate thickness of SEM< 80nm, a BET specific surface area of 28–30 m^2/g, and a bulk density of 0.2–0.3 g/cc.

Nanocomposites Preparation

Clay was mixed well with styrene monomer for achieving a good dispersion. Nanocomposites were synthesized by introducing different amounts of nano clay (1 phr, 2 phr, and 3 phr) into the unsaturated polyester (100 g). Nanoclay was dispersed in UP with the help of a high speed shear mixer for 15 min. This was followed by ultrasonication, for another 15 min, for improving the dispersion by breaking intermolecular interactions and also to get rid of any air bubbles. After mixing, cobalt naphthenate (1 phr) was added as accelerator and similarly methyl ethyl ketone peroxide (1 phr) was added as initiator and manually stirred. The mixture was then poured into Teflon molds and the samples were cured at room temperature for 24 h and later post cured at 80°C for 4 h.

Physical Measurements and Observations

Tensile Properties. Tensile properties of the samples are determined by Shimadzu Autograph AG-I Series Universal Testing Machine with a crosshead speed of 5 mm/min following ASTM D 638 standard. Dumbbell-shaped specimens were molded in Teflon molds with a length 165 mm, width 12.5 mm in the gauge section, and thickness of 4 mm.

Flexural Properties. A three-point loading system using UTM (Schimadzu AG-I) according to ASTM D 790 was used to determine the flexural properties of the UP/Clay nanocomposites. This test was performed at a crosshead speed of 5 mm/min using rectangular bars of dimensions 125 mm X 12.5 mm X 4 mm.

Impact Properties. It was determined using un notched samples with dimensions 62.5mm X 12.5 mm X 4 mm according to ASTM D 4812 on a Ceast Resil Impact Analyzer (Junior) using a hammer of 4 J at a striking rate of 3.96 m/s.

Dynamic Mechanical Analysis. The influence of nanoclay on the viscoelastic properties of polyester/kaolin clay was studied in detail using DMA Q-800, TA instruments. For this, rectangular shaped specimens with dimensions 62.5mm X 12.5 mm X 4 mm were prepared. In order to obtain dynamic storage modulus (E') and loss modulus (E"), a temperature sweep method was employed, where the temperature increases from 40°C to 125°C at 3°C/min, at a constant frequency of 1 Hz. Tan δ ($E"/E'$) was also calculated.

Thermal Stability. thermogravimetric analysis (TGA) Q-50, TA instruments under nitrogen atmosphere was utilized to analyze the thermal stability of the UP/kaolin clay by heating a sample of weight 5–7 mg at a rate of 20°C/min from room temperature to 800°C.

X-ray Diffraction Analysis (XRD). This analysis was done to find the change in basal spacing of nanocomposites. For this, the samples were analyzed in a Bruker AXS D8 Advance Powder Diffractometer that was equipped with Cu radiation. The samples were scanned in at 2θ range of 3°–80° at a wave length of 1.5406 Å. The scanning was done with an increment step of 0.020°.

Fourier Transform Infrared Spectroscopy (FTIR). Thermo Nicolet, Avatar 370 instrument was used for recording Fourier transform infrared spectra of the specimens.

Scanning Electron Microscopy (SEM). The morphology of the tensile fractured surfaces of the nanocomposite specimens was studied in detail using SEM. To achieve the necessary conductivity, the samples were gold sputtered before conducting electron microscopy. JEOL Model JSM 6390LV scanning electron microscope was used for this purpose.

Transmission Electron Microscopy (TEM). The formation of the nanocomposite specimens were further investigated in detail

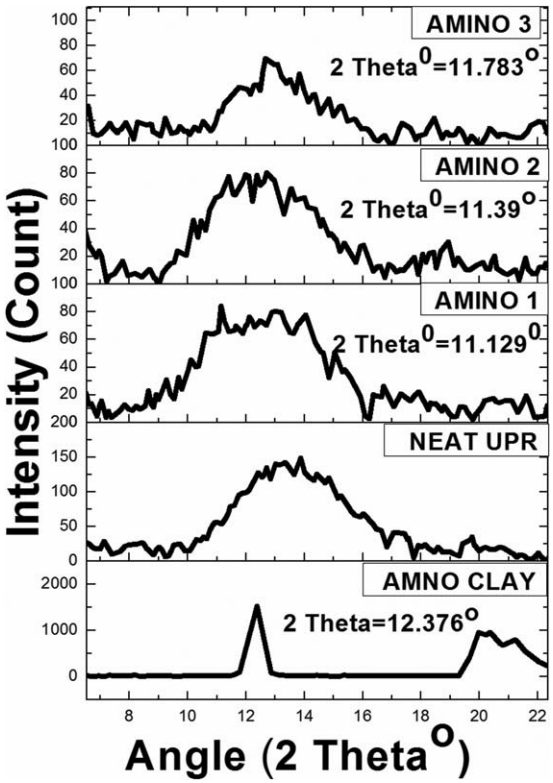

Figure 1. XRD patterns of Amino modified Clay and the UP composites with various loadings of Amino clay.

using Transmission Electron Microscopy. For this the amino-modified clay was dispersed in acetone using ultrasonicator and a drop of the dispersion was placed on carbon-coated 200 mesh copper grids and allowed to evaporate for TEM observation. Leica Ultracut UCT Ultramicrotome at room temperature helped in obtaining the ultra thin TEM sample of nanocomposite with a thickness of 70 nm. These microtomed thin sections were collected on 200 mesh copper grids and examined by a JEOL JEM 2100 High Resolution Transmission Electron operating at 200 kV acceleration voltages.

Dynamic Viscosity. Viscosities were determined at 25°C using RVT Brookfield Viscometer. The viscosity was investigated at 0, 1, 2, and 3 phr of clay with unsaturated polyester before curing.

RESULTS AND DISCUSSION

Morphology of Polymer Composite by XRD, FTIR, SEM, and TEM

X-ray Diffraction. X-ray diffraction method can confirm the dispersion of nanoclay in the composite, which is often used to clearly make out intercalated structures using Bragg's law of diffraction, $n\lambda=2d\sin\theta$, where λ represents the wavelength of the x-ray radiation used (λ =1.5405 Å), d is the spacing between diffraction lattice planes and θ, the diffraction angle. The d value corresponding to the (001) plane was used in this study.

The unsaturated polyester is well intercalated between platelets of amino modified clay. This causes an increase in the d-spacing of the clay lattice when compared with that of pure clay. Intercalation is evidenced by the change in the position, broadness, and intensity of the characteristic peak in XRD spectra. Increasing of d-spacing results in the broadening and shifting of related XRD peak toward lower diffraction angles (2θ) in accordance with Bragg law. Thus by monitoring position, shape, and intensity of the peak for organoclay in nanocomposite, it is possible to determine the degree of intercalation/exfoliation.[27,28]

Figure 1 shows the XRD patterns of Amino modified clay as well as unsaturated polyester nanocomposites containing 1, 2, and 3 phr amino modified clay. The characteristic peak of Amino modified clay has been appeared at $2\theta = 12.376°$ corresponding to the inter layer space of 0.71457 nm. This peak is overlapped with the broad peak of unsaturated polyester and the amorphus nature of the polyester is retained in the polymer nanocomposites. The peak is also shifted towards the lower angle (2θ) values 11.129°, 11.39°, and 11.783° which indicates the basal spacing of 0.79434 nm, 0.7762 nm, and 0.7504 nm, respectively. The lowering of the intensity of the characteristics peak of the amino modified clay is also observed in the XRD patterns. Increased value of d spacing of the amino modified nanoclay and lowering of the intensity of its characteristic peak along with the broadening indicate that the polymer chains are intercalated between the platelets of the nanoclay forming amorphous matrix of the polymer nanocomposites.

Fourier Transform Infrared Spectra (FITR). Figure 2 compares Fourier transform infrared spectra (FTIR) of amino modified clay, neat unsaturated polyester, and amino modified composite. An enlarged view of the spectra at around 3400 cm^{-1} for both amino modified 1 phr composite as well as for amino clay is also shown as in inset the Figure 2. It can be observed that the shoulder peak at 3400 cm^{-1} for amino modified clay is visible at the corresponding position in the composite spectrum, which is a clear indication of successful incorporation and distribution of modified clay nanoparticles in the matrix.

SEM. SEM is used to observe the fractured surface of the polymer composite obtained from tensile test. Figure 3(A) shows the fractured surface polyester composite with 2 phr of amino clay in which the surface shows a roughness where as in the

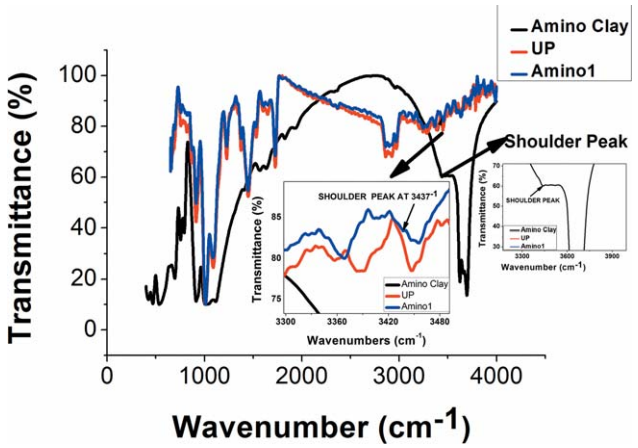

Figure 2. FTIR spectra of Amino Clay/UP/Amino1 composite. [Color figure can be viewed in the online issue, which is available at wileyonlinelibrary.com.]

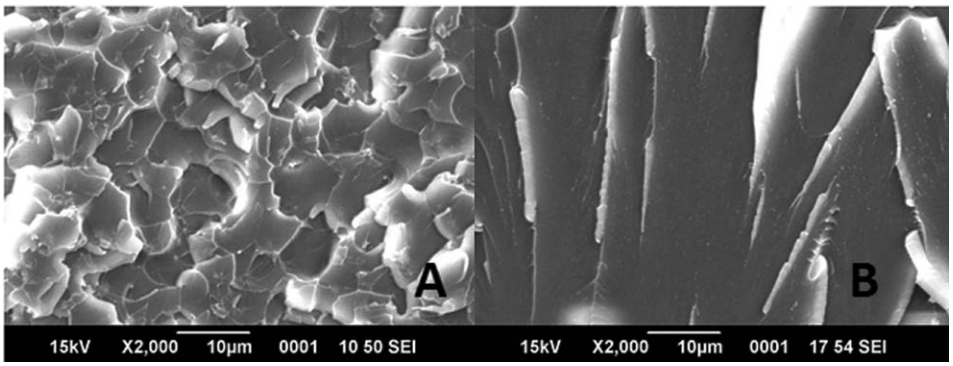

Figure 3. SEM of fractured surface of Neat UP and UP/clay composite (A) UP/Amino 2 X2000,10μm. (B) Neat UP X2000,10μm.

case of fractured surface of pure unsaturated polyester, which is featureless, typical of a glassy material as shown Figure 3(B). This happens due to the fact that the crack propagation is forced to take up a more tortuous path which increases the fracture surface area and the toughness. The nanoclay layers act as a barrier to the propagation of cracks.

TEM. Transmission electron microscopy (TEM) technique is utilized in this study to directly visualize the nanostructure of nanocomposites and clay d-spacing. They provide us a qualitative insight of the internal structure, the degree of exfoliation or spatial distribution of layers within the matrix. They also help in exhibiting the structural defects. Clay sheets are characterized by the occurrence of heavier elements like Al, Si, and O, while the main components such as C, H of the polyester are lighter in comparison. Hence in TEM micrographs, the darker lines in the brighter matrix denotes the presence of clay sheets, where as the brighter matrix denotes the polymer matrix, thereby provides an easy method to deduce the inter layer spacing of clay sheets in the matrix. Thus the distance between darker line sections can qualitatively show the dispersion status.[28]

Figure 4(A) represent the TEM image for 1phr amino clay modified UP nanocomposite at 500 nm and in Figure 4(B) represent same composite but showing dimensions of amino clay particles marked in nm thus showing that the dispersion of amino modified clay is in nanorange. The Figure 4(A) also shows that for 1 phr of amino modified clay composite nanoclay is uniformly dispersed in the matrix. Figure 4(C) represents TEM image of 2 phr amino modified clay composite and Figure 4(D) represents TEM image for 3 phr amino modified clay composite. Figure 4(C,D) clearly shows the agglomeration of nanoparticles which increases from 2 phr to 3 phr. Agglomeration of filler particles is clearly seen in TEM image of the 2 phr and 3 phr amino modified clay composite.

Thermal Stability

TGA has been used to study the thermal stability of the nanocomposites in nitrogen atmosphere. Percentage weight retention at various temperatures is given in Table I. It has been found that % weight retention increases with temperature for all ranges of temperature from 200°C to 600°C. Thus, thermal stability of the composite increase with the clay content in all range of temperature 200°C–600°C. Figure 5 shows TGA curves of UP and UP/Clay composites. The peak in the first derivative curve shows the point of maximum rate of change on the weight loss curve and is defined as the inflection point. The inflection point is also increase from 1 phr to 3phr of clay addition. The extrapolated onset temperature (T_o) that denotes the temperature at which the weight loss begins also increases when amino modification of clay change from 1 phr to 3 phr. Intercalated nanoclay platelets dispersed throughout the matrix act as barrier to heat and resistant to volatile degradation products. The inorganic platelets aid in the formation of char on the surface of the nanocomposite, which prevents any further thermal decomposition and raises the barrier for the escape of degradation products from the bulk. The restricted escape of degradation products thus enhances thermal stability of the composite.[29]

Dynamic Viscosity

The viscosity was investigated at 0, 1, 2, and 3 phr of clay with unsaturated polyester before curing. Viscosity of the polyester

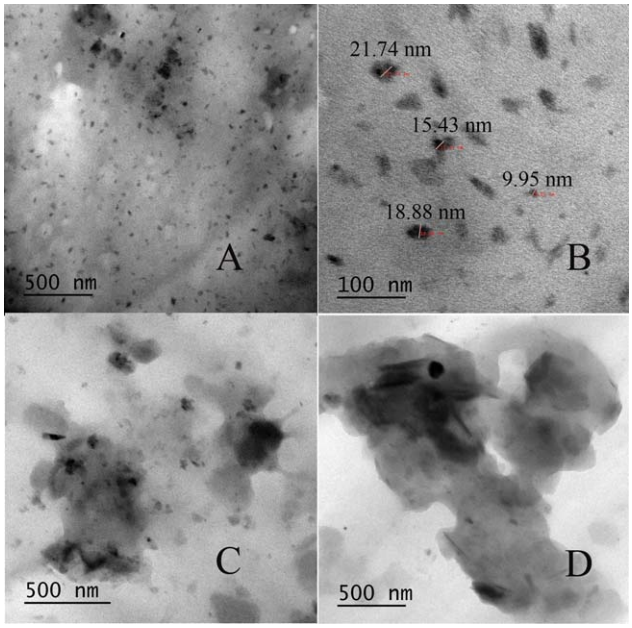

Figure 4. TEM of fractured surface of UP/clay composite (A) UP/AMINO1 500 nm (B) UP/AMINO1 100 nm (C) UP/AMINO2 500 nm (D) UP/AMINO3 500 nm. [Color figure can be viewed in the online issue, which is available at wileyonlinelibrary.com.]

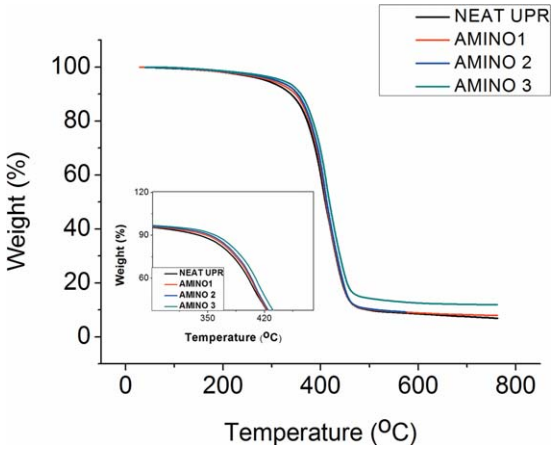

Figure 5. TGA curves of Neat UPR, Amino 1, Amino 2, and Amino3. [Color figure can be viewed in the online issue, which is available at wileyonlinelibrary.com.]

resin and mixtures of polyester resin with varying phr of clay was determined using RVT dial gauge Brookfield Viscometer at 25°C.The change in viscosity for 3 phr nanoclay addition when comparing with neat resin is 191%.The change viscosity with addition of nanoclay is shown in the Figure 6. The increase of viscosity is due to intercalation of polymer layers into the nanoclay.

Mechanical Properties

Dynamic Mechanical Behavior. The viscoelastic behaviour patterns of polymers are studied using dynamic mechanical analysis (DMA). The storage modulus (E′) values at temperatures of 45°C, 60°C, 80°C, 100°C, and 120°C are reported in Table II where in tanδ peak height and T_g in °C are also listed.

On evaluating Table II, it can be concluded that as the filler content increases in the composite, storage modulus values keep on increasing steadily. The nanocomposite with 3phr amino modified clay has 38% increase in storage modulus than that of neat UP at 45°C. Intercalation of polymer into clay layers and also the higher aspect ratio of clay platelets are the reason for this behaviour. Another important point to be noted is that

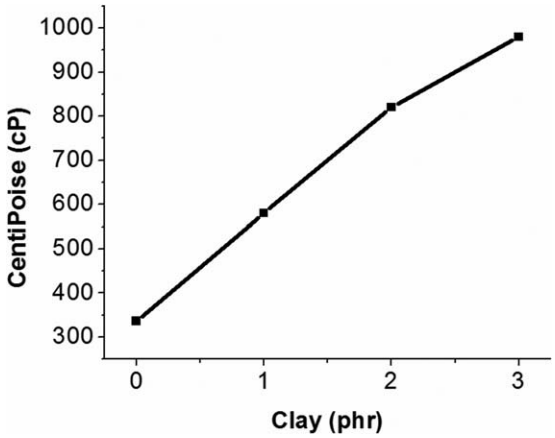

Figure 6. Change of Viscosity of the polyester with the addition of 1, 2, and 3 phr of clay.

Table I. Percentage of Weight Retention at Various Temperature, Residue at 750°C, Inflection Point (°C), Onset Temperature (°C) From TGA Thermograms of UP, and UPR/Clay Nano Composites

Aminoclay Phr	% of weight retention at various temperatures								Residue at 750°C	Inflection point °C	Onset temperature °C
	200°C	250°C	300°C	350°C	400°C	450°C	500°C	550°C	600°C			
0	98.1	96.73	94.25	87.82	60.07	16.8	9.95	9.085	8.568	7.035	402.44	331.73
1	98.14	96.98	94.91	89.67	62.6	17.1	10.21	9.414	8.908	8.001	407.52	332.7
2	98.38	97.35	95.53	90.68	64.24	17.66	10.41	9.54	8.976	8.718	408.38	334.6
3	98.58	97.65	96.15	91.98	69	22.33	14.31	13.24	12.56	11.94	411.87	339.34

Table II. Storage Modulus and T_g of the UPR/Clay Nanocomposites, Estimated by DMA

Amino clay phr	Storage modulus (Mpa)					Tan ∂ Peak height	T_g °C
	45°C	60°C	80°C	100°C	120°C		
0	956.7	445.1	53.32	12.49	9.21	0.4294	83.08
1	1100	928.4	466.8	132.5	31.07	0.36505	108.89
2	1277	1108	580	181.3	40.2	0.38158	109.96
3	1328	1190	725.2	264.4	49.36	0.43177	114.62

tanδ peak height value is the lowest for 1phr of amino clay, which shows better reinforcement of the matrix at that filler loading. Here the decrease in the tanδ values is due to the restrictions imposed by the intercalated and uniformly distributed nano clay, against molecular motion of polymer chains resulting in better elastic response of the material. Increase of tanδ at higher loadings of nanoclay may be due to some amount of agglomeration of the filler in the composite. It is also observed from Table II that the glass transition of the composites shifts to higher temperatures as the filler content increases, which indicates the reinforcement effect of nanoclay.

Variation of storage modulus, loss modulus, and tan delta, of the composites, in a temperature range of 45°C–125°C are given in Figure 7(A–C), respectively. As shown in Figure 7(A), storage modulus of the composite with 3 phr clay loading is higher for the entire range of temperatures in comparison with that of 2 phr and 1 phr composite. Loss modulus also increases with increase of clay content of the composite as shown in Figure 7(B). This may be due to the dissipation of energy at the matrix-particle interface, which increases with the clay content. As shown in Figure 7(C), tanδ peak shifts towards higher temperatures as filler content increases indicating the reinforcement offered by nanoclay.

Variation in relative storage modulus of nanocomposites with different filler loadings is shown in Figure 7(D). Relative storage modulus can be calculated by taking the ratio of $E'_{UP/CLAY}$ and E'_{UP}. On analyzing the graph, it is clearly noted that the relative storage modulus is maximum for 3 phr clay nanocomposite and it increases in the order 1 phr to 3 phr.

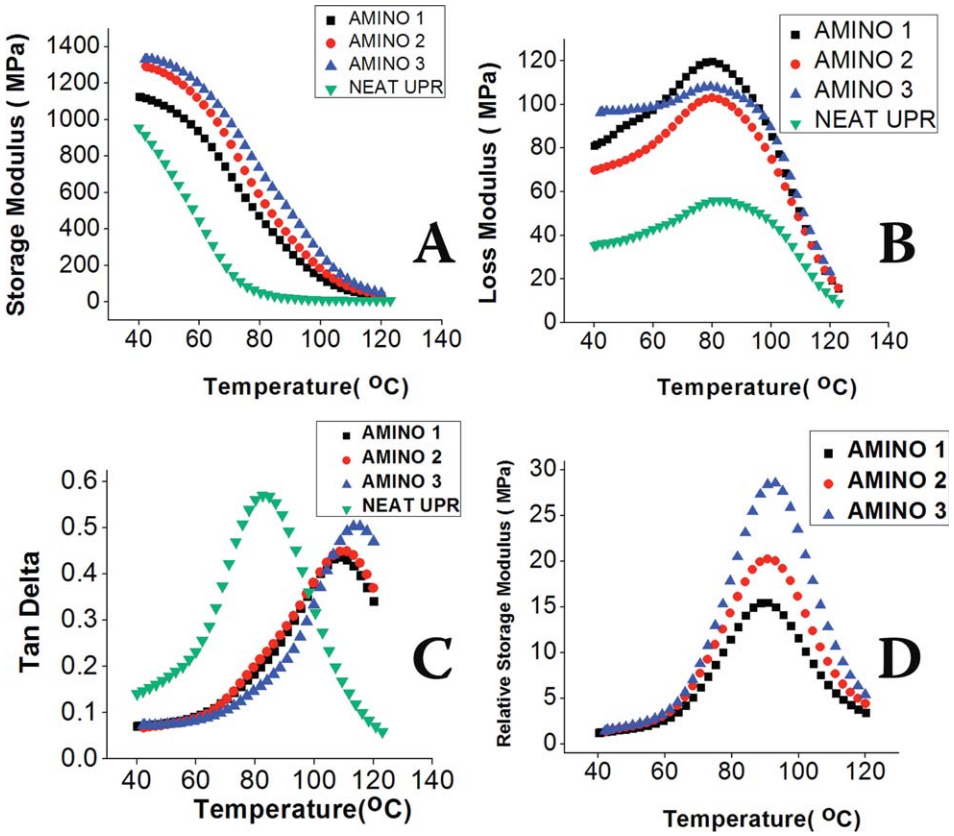

Figure 7. Variations of storage modulus (A) loss modulus (B) tan δ (C) of UP composites from 1 phr, 2 phr, and 3 phr Amino clay loadings with Temperature. (D) Variation of relative storage modulus with different nanoclay composition. [Color figure can be viewed in the online issue, which is available at wileyonlinelibrary.com.]

The curves are "hump-like," which can be explained by the hindrance of polymer chain movement attributed to the clay particles within them, happens because of the resistance of the applied stress on account of development of polymer nanoclay network, which in turn increases with nanoclay loadings, thereby increasing the size of the so-called "hump-like curves.[30,31]

Mechanical Properties. Introduction of nanomodified clay into UP considerably improves the mechanical behaviour of the composites. Typical stress strain curves of neat UP and its composites at various clay loadings are shown in the Figure 8.

As shown in Figure 8, the slope of the curves in the stress strain graph keeps on increasing with nanoclay content indicating increase of tensile modulus. This is in correspondence with Figure 9(A), where variation of tensile modulus is plotted against nanoclay content. As seen in Figure 9(B), at 1 phr of nanoclay content tensile strength of the composite is maximum. At higher filler loadings tensile strength goes on decreasing. This may be due to the agglomeration of filler particles at higher loadings. Agglomeration of filler particles is evident in the Figure 4 of TEM image of the 2 phr and 3 phr clay composite.

As shown in Figure 9(C) strain at break also follows a similar trend as that of the tensile strength, with 1 phr composites showing maximum strain. From the tensile measurements it can be inferred that reinforcement is most effective at 1 phr nanoclay content. Flexural modulus of the composite increases in the order of increasing filler content as clearly indicated in the Figure 9(D).

Toughness is defined as the capacity of a material to absorb energy and deform plastically without fracturing and is measured by the area under the stress strain curve of the material. Toughness value of the composites is found to be maximum for 1 phr of clay as show in Figure 9(E). Toughness decreases when clay content is further increased. More energy is required for overcoming the reinforcement offered by the finely dispersed nanoclay particles. At higher loadings agglomeration of the nanoparticles decreases the reinforcement thus decreasing the toughness.

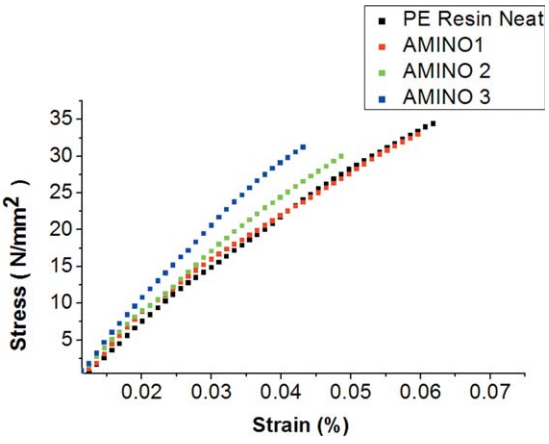

Figure 8. Stress–Strain curve extracted from tensile test of nanocomposite with various clay loading. [Color figure can be viewed in the online issue, which is available at wileyonlinelibrary.com.]

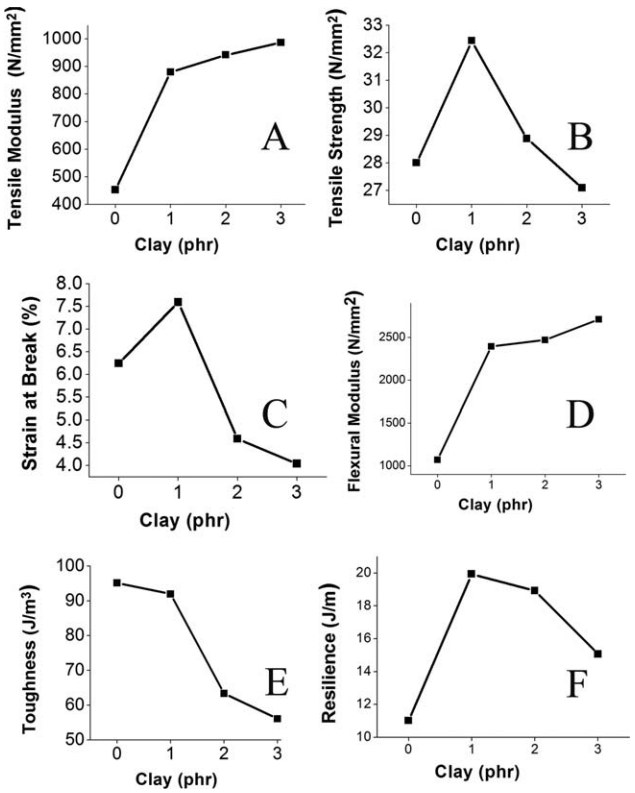

Figure 9. Variations of tensile modulus (A), tensile strength (B), strain at break (C), flexural modulus (D), toughness (E), and resilience (F) of UP composites from 1 phr, 2 phr, and 3phr amino clay loadings with temperature.

Resilience is defined as the capability of a material to absorb energy when it is deformed elastically and to discharge that energy when it is unloading. Materials with high resilience can withstand bending and straightening without damage. Resilience of the neat resin and nanoclay composites was measured using un-notched samples in an Impact tester. Composites with 1 phr clay have the maximum resilience as shown in the Figure 9(F). Improved reinforcement at this filler loading makes the composite more resilient. On further addition of fillers, resilience kept on decreasing.

CONCLUSIONS

Investigations have been made on the mechanical and thermal behavior of unsaturated polyester composite. The better dispersion of unsaturated polyester composite with amino-modified kaolin clay can be achieved with mechanical stirring and ultrasonication. The intercalated structure of thus formed amino silane modified nanocomposite shows a much superior mechanical and thermal properties as expected. They also possessed other properties like higher storage modulus and loss modulus than the neat polyester. Thermal stability of the modified clay has been studied with the help of TGA and is shown that the thermal stability improved the addition of modified clay.

Better dispersion of nanoclay particles in polyester matrix has clearly been shown with the help of morphological studies. XRD spectrum clearly demonstrates the delamination of amino modified clay layers in the nanocomposite. FTIR Spectra of amino modified clay, neat unsaturated polyester, and amino modified composite corroborates the incorporation and distribution of modified nanoclay particles in the matrix. Also, the TEM and SEM images of UP/amino modified nanocomposite clay verify the well intercalated structure, which can be responsible for its superior thermal stability and dynamic mechanical properties. Regarding storage modulus, nanocomposites with 3 phr modified clay shows 38% higher storage modulus than that of neat UP/clay composite.

The SEM of fractured surface of pure unsaturated polyester and that of composite with nanoclay is also investigated and it has been found that the fractured surface of pure unsaturated polyester was featureless, where as in case of composite with nanoclay, the surface showed a roughness. Here the crack propagation is forced to take up a more tortuous path which increases the fracture surface area and thereby the toughness. Also, introduction of nano modified clay into UP significantly improves the tensile properties of the composite. Tensile strength was found to be maximum for 1 phr filler loading. Similarly resilience of the composites also follows a similar trend. With respect to tensile modulus properties, it kept on increasing with the filler content. TEM images also show an even distribution of clay for 1 phr. This is also in agreement with the finding of maximum tensile strength at 1 phr. With high phr of clay, agglomeration of clay particle happens and it is clearly evident by TEM image and as a result, tensile strength also lowers.

REFERENCES

1. Barbe, P.; Balasubramanian, S.; Anguchamy, Y.; Gong, S.; Wibowo, A.; Gao, H.; Ploehn, H. J.; Loye, H. C. *J. Materials* **2009**, *2*, 1697.
2. Kang, X.; Zhang, W.; Yang, C. *J. Appl. Polym. Sci.* **2016**, *133*, DOI: 10.1002/app.42869.
3. Choudhury, M.; Mohanty, S.; Nayak, S. K.; Aphale, R. *J. Miner. Mater. Charact. Eng.* **2012**, *11*, 744.
4. Hasegawa, G.; Shimonaka, M.; Ishihara, Y. *J. Appl. Toxicol.* **2012**, *32*, 72.
5. Sharma, R. A.; D'Melo, D.; Bhattacharya, S.; Chaudhari, L.; Swain, S. *Trans. Electr. Electron. Mater.* **2012**, *13*, 31.
6. Kojima, Y.; Usuki, A.; Kawasumi, M.; Okada, A.; Fukushima, Y.; Kurauchi, T.; Kamigaito, O. *J. Mater. Res.* **1992**, *8*, 1185.
7. Kornmann, X.; Berglund, L. A.; Sterte., J.; Giannelis, E. P. *Polym. Eng. Sci.* **1998**, *38*, 1351.
8. Yano, K.; Usuki, A.; Okada, A.; Kurauchi, T.; Kamigaito, O. *J. Polym. Sci. Part A: Polym. Chem.* **1993**, *31*, 2493.
9. Kojima, Y.; Fukumori, K.; Usuki, A.; Okada, A.; Kurauchi, T. *J. Mater. Sci. Lett.* **1993**, *1212*, 889.
10. Kelly, P.; Akelah, A.; Qutubuddin, S.; Moet, A. *J. Mater. Sci.* **1994**, *29*, 2274.
11. Haque, E.; Armeniades, C. D. *Polym. Eng. Sci.* **1986**, *26*, 1524.
12. Giannelis, E. P. *Adv. Mater.* **1996**, *8*, 29.
13. Lee, J.; Takekoshi, T.; Giannelis, E. P. *MRS Proc.* **2011**, *457*, 513.
14. Fu, X.-A.; Qutubuddin, S. *Polym. Eng. Sci.* **2004**, *44*, 345.
15. Rashid, E. S. A.; Ariffin, K.; Kooi, C. C.; Akil, H. M. *Mater. Des.* **2009**, *30*, 1.
16. Hossain, M. E.; Hossain, M. K.; Hosur, M. V.; Jeelani, S. *J. Eng. Mater. Technol.* **2015**, *137*, 031005.
17. Bensadoun, F.; Kchit, N.; Billotte, C.; Trochu, F.; Ruiz, E. *J. Nanomater.* **2011**, *2011*, 1.
18. Krishnan, A. K.; George, T. S.; Anjana, R.; Joseph, N.; George, K. E. *J. Appl. Polym. Sci.* **2013**, *127*, 1409.
19. Krishan, A. K.; George, K. E. *Polym. Adv. Technol.* **2014**, *25*(9), 955.
20. Bagherpour, S. Polyester; Saleh HE-D., Ed.; InTech:, **2012**; Chapter 6, p 142, DOI: 10.5772/2748.
21. Letaief, S.; Diaco, T.; Pell, W.; Gorelsky, S. I.; Detellier, C. *Chem. Mater.* **2008**, *20*, 7136.
22. Cheng, H.; Liu, Q.; Yang, J.; Zhang, Q.; Frost, R. L. *Thermochim. Acta* **2010**, *503504*, 16.
23. Alexandre, M.; Dubois, P. *Mater. Sci. Eng. R Reports* **2000**, *28*, 1.
24. Mittal, V. *Materials (Basel)* **2009**, *2*, 992.
25. Zhu, Y.; Ma, H.-Y.; Tong, L.-F.; Fang., Z.-P. *J. Zhejiang Univ. Sci. A* **2008**, *9*, 1614.
26. Ray, S. S.; Pouliot, S.; Bousmina, M.; Leszek, A.; Utracki, *Polym.* **2004**, *45*, 8403.
27. Hemmasi, A. H.; Ghasemi, I.; Bazyar, B.; Samariha, A. *BioResources* **2013**, *8*, 3791.
28. Olad, A. Advances in Diverse Industrial Applications of Nanocomposites; Reddy, B., Ed.; InTech:, **2011**; Chapter 7, p 124.
29. Sharma, S. K.; Nayak, S. K. *Polym. Degrad. Stab.* **2009**, *94*, 132.
30. Chafidz, A.; Ali, M. A.; Elleithy, R. *J. Mater. Sci.* **2011**, *46*, 6075.
31. Hasegawa, N.; Okamoto, H.; Kato, M.; Usuki, A. *J. Appl. Polym. Sci.* **2000**, *78*, 1918.